Splitting Approach to Coupled Navier-Stokes and Molecular Dynamics Equations

Jürgen Geiser[1]

Abstract

In this paper, we present a multi-scale method with a splitting approach based on iterative operator splitting methods, which takes into account the disparity of the macro- and microscopic scales. We couple the Navier–Stokes and the Molecular Dynamics equations, while taking into account their underlying scales. The underlying ideas are to save computational costs by decoupling complicated systems. Combining relaxation methods and averaging techniques we can optimize the computational effort. The motivation arose from modeling fluid transport under the influence of a multiscale problem, which has to be solved with smaller time scales, e.g., non-Newtonian flow problem. The applications include colloid damper or fluid–solid problems, where we study an area where the Navier–Stokes equations have less information about the stream field and we need at least the Boltzmann equation to obtain enough information about the whole density field. A novel research field is, e.g., Carbon Nanotubes, where we have to couple macro- and micromodels and obtain a fluid–solid area which uses the Lennard–Jones fluid model.

[1] Ernst-Moritz-Arndt Univeristy Greifswald, Institute of Physics,
  Felix-Hausdorff-Str. 6, D-17489 Greifswald, Germany,
  e-mail: juergen.geiser@uni-greifswald.de

The proposed method for solving such delicate problems enables simulations in which the continuum flow aspects of the flow are described by the Navier–Stokes equations at time-scales appropriate for this level of modeling, while the viscous stresses within the Navier–Stokes equations are the result of Molecular Dynamics simulations, with much smaller time-scales. The main benefit of the proposed method is that the time-dependent flows can then be modeled with a computational effort which is significantly smaller than if the complete flow were to be modeled at the molecular level, as a result of the different time-scales at the continuum and molecular levels, enabled by the application of the iterative operator-splitting method.

We discuss the convergence analysis of these splitting methods, see also [26].

Finally we present numerical results for the modified methods and applications to real-life flow problems.

1   Introduction

We motivate our study of combining multiple scale problems with time-decomposition methods. In the last few years, the solving of multi-scale problems has been a large topic. Solver methods to couple large scales are important, see [18] for lattice Boltzmann models, [2] for fluid dynamical problems. Numerically, the delicate coupling of continuous and discrete levels is discussed in [24].

In our paper we concentrate on optimizing the coupling process using a new method called iterative splitting. Iterative and relaxed splitting methods have their benefits in coupling time-scales, see [11] and [10]. For coupling the

Navier–Stokes equations and the equations of Molecular Dynamics, which involve different time-scales, one can employ averaging and density ideas, see [2]. Here we present different algorithmic schemes to accelerate the solver process. We propose a new idea in considering splitting methods as simultaneous coupling schemes, and consider the benefits of replacing expensive MD simulations with a a micro-scale viscous flux, which can be embedded into fixed point iteration schemes.

This paper is organized as follows. The mathematical model based on the coupled Navier–Stokes and molecular dynamical equations is introduced in Section 2. The iterative splitting method for the nonlinear equation is given in Section 3. The computation of the molecular-level shear stress is given in Section 4. The implicit dual-time stepping method is discussed in Section 5. We introduce the numerical results in Section 6. Finally we discuss perspectives for future research in the area of splitting and decomposition methods for multi-scale problems.

2 Mathematical Model

Our model equations come from fluid dynamics.

The macro-scale equation is given by the Navier–Stokes equation for incompressible continuum flow:

$$\rho \partial_t u + \rho (u \cdot \nabla) u - \mu \Delta u + \nabla p = \rho \, f, \text{in} \Omega \times (0, T), \tag{1}$$

$$\nabla \cdot u = 0, \text{in} \Omega \times (0, T), \tag{2}$$

$$u(0) = u_0, \text{on} \Omega,$$

$$u = 0, \text{on} \partial \Omega \times (0, T),$$

The unknown flow vector $u = u(x, t)$ is assumed to lie in $\Omega \times (0, T)$. In the above equations, ρ and p represent the fluid density and pressure, respectively. Here, μ represents the dynamic viscosity of the fluid. In the momentum equation, i.e., Equation (1), the term f on the right-hand side represents a volume source term. Equation (2) constrains the velocity field to be divergence-free, which is consistent with the assumption of incompressible flow.

The microscopic equation is given by Newton's equation of motion for each individual molecule i for a sample of N molecules,

$$m_i \partial_{tt} x_i = F_i, i = 1, \dots, N, \tag{3}$$

where F_i denotes the force acting on each molecule, and is the result of the inter-molecular interaction of molecule i with the neighboring molecules within a finite interaction range. In the present paper, we assume that the inter-particle forces are based on the well-known Lennard–Jones interaction potential [20], i.e., we assume the the microscopic flow is that of a Lennard–Jones fluid, details of which are given in a later section.

The coupling between the macro-scale equation (1) and micro-scale equation (3) is assumed to take place through the exchange of the viscous stresses in the momentum equation (1). The underlying idea is to replace the viscous stresses based on the continuum Newtonian equations in Equation (1) with a viscous stress evaluated by Molecular Dynamics simulations of the micro-scale fluid with the velocity gradient at macro-scale level imposed on the micro-scale fluid, through the use of Lees–Edwards boundary conditions [19]. The molecular-level viscosity is evaluated using the Irving–Kirkwood relation [15].

The viscous stress contribution $\mu \Delta v$ in Equation (1) can be generalized for a non-Newtonian flow to be $\partial \sigma_{ij}/\partial x_j$, using Einstein's summation convention. In the present paper, this non-Newtonian viscous stress contribution is reformulated in the following form.

$$\partial \sigma_{ij}/\partial x_j = \mu_{apparent} \partial^2 v_i / \partial x_j^2 \tag{4}$$

where the 'apparent' viscosity can be a general function of the imposed velocity gradients in each spatial direction, i.e., this expression can represent general non-continuum and non-Newtonian flow conditions. The viscous stresses in Equation (1) can now be replaced by molecular level viscous stresses by introducing a constant approximate viscosity μ_{approx} and taking into account the deviation of the molecular-level viscous stresses from this approximate viscosity through a volumetric source term.

Finally, we obtain the coupled multi-scale equations:

$$\rho \partial_t v + \rho (v \cdot \nabla) v - \mu_{approx} \Delta v + \nabla p = f, \text{in} \Omega \times (0, T), \tag{5}$$
$$f_i = \partial \sigma_{ij}/\partial x_j |_{molecular} - \mu_{approx} \Delta v_i$$

where Einstein's summation convention is used for the volumetric source term f, which accounts for the deviation of the viscous stresses evaluated at the molecular level from the approximate Newtonian relation $\mu_{approx}\Delta v$. The molecular-level viscous stresses can be further reformulated using the apparent viscosity, as demonstrated in Equation (4).

3   Iterative Splitting Method

The following algorithm is based on an iteration with fixed splitting discretization step-size τ. The splitting scheme can be formulated as a predictor corrector scheme or as a three steps method. On the time interval $[t^n, t^{n+1}]$, we solve the following sub-problems consecutively for $i = 1, 2, \ldots M$.

$$\frac{\partial c_i(t)}{\partial t} = Ac_i(t) \ + \ Bp_{i-1}(t), \text{ with } c_i(t^n) = c^n \tag{6}$$

$$i = 1, 2, \ldots, j \ , \tag{7}$$

$$Bp_{i+1}(t) = f(c_i) \ , \tag{8}$$

$$i = j + 1, j + 2, \ldots, m \ , \tag{9}$$

$$\frac{\partial c_{i+2}(t)}{\partial t} = Ac_i(t) \ + \ Bp_{i+1}(t), \text{ with } c_{i+2}(t^n) = c^n \tag{10}$$

$$i = m + 1, m + 2, \ldots, M \ , \tag{11}$$

where we assume the operator A has a large time scale and B has a small time scale.

Here we decouple the different time-scales and stabilize the scheme with averaging functions f.

Theorem 3.1. *Let us consider the abstract Cauchy problem in a Banach space* **X***:*

$$\partial_t c(t) = Ac(t) + Bp(t), \quad 0 < t \leq T, \tag{12}$$

$$Bp = f(c), \tag{13}$$

$$c(0) = c_0, \tag{14}$$

where $A, B, A + B : \mathbf{X} \to \mathbf{X}$ are given linear operators which generate the C_0-semigroup, and $c_0 \in \mathbf{X}$ is a given element. Then the iteration process (6)–(8) is convergent and the rate of the convergence is of higher order.

The proof can be found in [11].

In more detail, we can consider the iterative operator splitting method as a waveform relaxation form with multiple steps. This helps to understand the algorithmic implementation of the schemes, see applications in [21].

So let us consider the following scheme.

Waveform Relaxation Method:

$$\frac{du_i}{dt} = Pu_i + Qu_{i-1} + f, \tag{15}$$

$$u_i(t^n) = u(t^n), \tag{16}$$

where $A = P + Q$, e.g., P is the diagonal part of A (Jacobi method).

Here, the splitting method is made abstractly with respect to the matrix A. This method is considered an effective solver method with respect to the underlying matrices.

Iterative Operator Splitting Method:

$$\frac{du_i}{dt} = Pu_i + Qu_{i-1} + f, \tag{17}$$

$$u_i(t^n) = u(t^n), \tag{18}$$

$$\frac{du_{i+1}}{dt} = Pu_i + Qu_{i+1} + f, \tag{19}$$

$$u_{i+1}(t^n) = u(t^n), \tag{20}$$

where P, Q are matrices given by spatial discretization, e.g., P is the convection part of Q the diffusion part.

But we can also perform an abstract decomposition, take into account $A = P + Q$, where P is a matrix with small eigenvalues and Q is a matrix with large eigenvalues.

4   Molecular-Level Shear Stress Computation

In the present paper, the microscopic model is given by Newton's equations for the motion of the individual molecules, for which the well-known Molecular Dynamics (MD) method [1] is used. The MD method simulates the dynamics of a system of N interacting molecules by temporal integration of Newton's equations of motion, for which the velocity Verlet algorithm [27], which is second-order accurate in time, is used,

$$
\begin{aligned}
\underline{x}_i^{(n+1)} &= \underline{x}_i^{(n)} + \delta t \underline{v}_i^{(n)} - \frac{\delta t^2}{2m_i} \nabla U_i^{(n)} \qquad i = 1, \ldots, N \\
\underline{v}_i^{(n+1)} &= \underline{v}_i^{(n)} + \frac{\delta t}{2m_i} \nabla U_i^{(n)} \qquad i = 1, \ldots, N
\end{aligned}
\tag{21}
$$

In the present paper, the Lennard–Jones fluid is used as a model, i.e., an atomic medium with an inter-particle potential given by

$$
U_{LJ}(r_{ij}) = 4\epsilon_{ij}\Big[\Big(\frac{\sigma_{ij}}{r_{ij}}\Big)^{12} - \Big(\frac{\sigma_{ij}}{r_{ij}}\Big)^{6} \Big],
\tag{22}
$$

where r_{ij} is the distance between particles i and j, ϵ_{ij} is the depth of the potential well, and σ_{ij} is the (finite) distance greater than which the inter-particle potential becomes zero. The Lennard–Jones potential combines a strong repulsion at short distances with a weak attraction at longer distances. In the above equation, σ_i as well as ϵ_i are assumed identical for $i = 1, \ldots, N$. Furthermore, a cut-off distance r_c is defined.

To model hydrodynamics using the MD method, the following steps are typically employed. First, a number of microscopic domains are initialized with randomly-placed particles with a the number density consistent with the pre-scribed fluid density. Secondly, using an appropriate time-integration method, coupled with a thermostat to control the temperature, the microscopic solutions are integrated for a sufficiently long time to reach an equilibrium solution at the prescribed density and temperature. Following this initial equilibration phase, the microscopic equations are further integrated in time. In this phase, the particle positions and velocity are used to perform an averaging in space and time, as well as ensemble averaging when multiple microscopic solutions are considered.

Figure 1 presents the results from a large number of Molecular Dynamics simulations for a cubic domain of dimension 12σ with a 1382 particles, i.e.,

the density in Lennard–Jones units is 0.8. For a range of velocity gradients imposed linearly on this domain, the shear stresses are presented. The results are compared for ensemble averaging over 4, 8 and 16 independent realizations and for sampling durations of 100τ and 200τ. The time-steps in the MD simulations are 0.001τ.
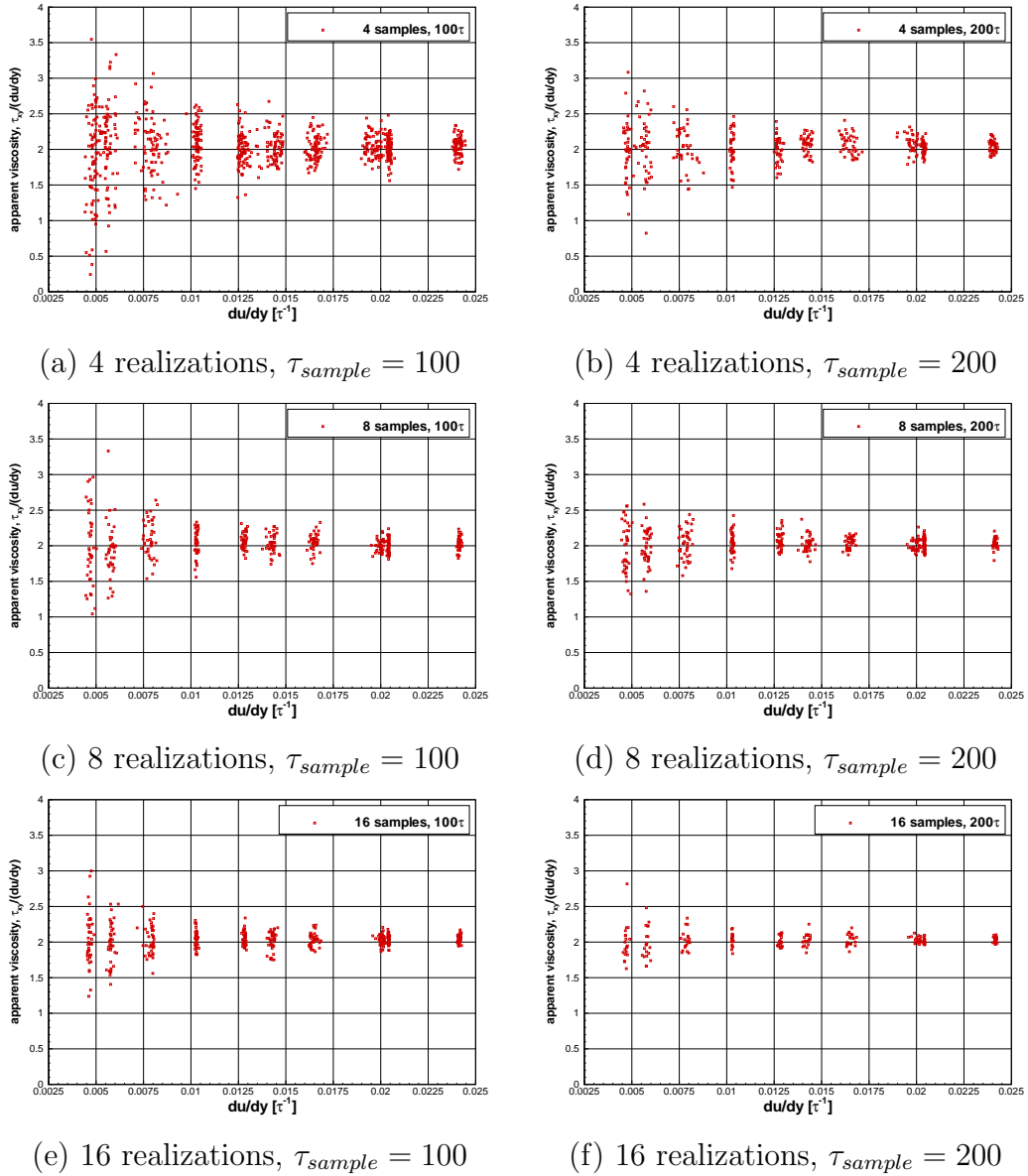

(a) 4 realizations, $\tau_{sample} = 100$ (b) 4 realizations, $\tau_{sample} = 200$

(c) 8 realizations, $\tau_{sample} = 100$ (d) 8 realizations, $\tau_{sample} = 200$

(e) 16 realizations, $\tau_{sample} = 100$ (f) 16 realizations, $\tau_{sample} = 200$

Figure 1: Effect of the number of independent realizations and sampling duration on the statistical scatter in the predicted apparent viscosity. Lennard–Jones fluid at $0.80\sigma^{-3}$ and $T = 1.50$.

5 Implicit Dual-Time Stepping Method for Time-Dependent Flows

We start with a first example to use the stable first order splitting as a pre-step method and then start with the higher order iterative method.

5.1 Governing equations for macro-scale and micro-scale problems

The Navier–Stokes equations written in integral form for a domain fixed in time are

$$\frac{d}{dt}\int_{V(t)} \vec{w}dV + \int_{\partial V(t)} \big(\vec{F}(\vec{w}) - \vec{F}_v(\vec{w})\big)\vec{n}dS \;=\; \vec{S}. \tag{23}$$

They form a system of conservation laws for any fixed control volume V with boundary ∂V and outward unit normal $\vec{n}$. The vector of conserved variables is denoted by $\vec{w} = [\rho, \rho u, \rho v, \rho w, \rho E]^T$, where ρ is the density, u, v, w are the Cartesian velocity components, and E is the total internal energy per unit mass. $\vec{F}$ and $\vec{F}_v$ are the inviscid and viscous flux, respectively. In the absence of volume forces and in an inertial frame of reference, the source term $\vec{S} = 0$.

Assuming that the x-direction is the homogeneous direction, the y direction is the cross-flow direction, and that the flow is incompressible with vanishing velocity components in the y and z directions, the governing equation can then be rewritten as

$$\rho\partial u/\partial t - \mu_{approx}\partial^2 u/\partial x^2 + \partial p/\partial x = f, \tag{24}$$
$$f = \partial\sigma_{xy}/\partial x - \mu_{approx}\partial^2 u/\partial x^2$$

using the multi-scale Equation (5).

Equations (23) are discretized using a cell-centered finite volume approach on structured multi-block grids, which leads to a set of ordinary differential equations in time of the form

$$\frac{\partial}{\partial t}\big(\mathbf{w}_{i,j,k}V_{i,j,k}\big) \;=\; -\mathbf{R}_{i,j,k}\big(\mathbf{w}_{i,j,k}\big) \tag{25}$$

where $\mathbf{w}$ and $\mathbf{R}$ are the vectors of cell variables and residuals, respectively. Here, i, j, k are the cell indices in each block and $V_{i,j,k}$ is the cell volume.

In the present paper, the flow problems considered lead to a reduction of the full Navier–Stokes equations to a set of equations for the velocity field components. Hence, the vector $\mathbf{w}$ in this paper only involves the Cartesian velocity components, while $\mathbf{R}$ represents the residuals of the three moment equations.

Boundary conditions are imposed by using two layers of halo cells around each grid sub-domain. Zero-slip conditions at the solid walls are imposed by extrapolating the halo cell values in such a way that the velocity at the wall vanishes.

5.2   Dual-time stepping method

For time-accurate simulations, the temporal integration is performed using an implicit dual-time stepping method. Following the pseudo-time formulation [16], the updated mean flow solution is calculated by solving the steady state problems

$$\mathbf{R}^*_{i,j,k} \;=\; V_{i,j,k}\frac{3\mathbf{w}^{n+1}_{i,j,k} - 4\mathbf{w}^n_{i,j,k} + \mathbf{w}^{n-1}_{i,j,k}}{2\Delta t} + \mathbf{R}_{i,j,k}\big(\mathbf{w}^{n+1}_{i,j,k}\big) = 0. \qquad (26)$$

Equation (26) is a nonlinear system of equations for the full set of Navier–Stokes equations. However, for the reduced system of equations resulting from the homogeneity and periodicity assumptions, presented in Equation (24), this system of equations is actually linear. This system is solved by introducing an iteration through *pseudo time* τ to the steady state, as given by

$$\frac{\mathbf{w}^{n+1,m+1}_{i,j,k} - \mathbf{w}^{n+1,m}_{i,j,k}}{\Delta \tau} + \frac{3\mathbf{w}^{n+1,m}_{i,j,k} - 4\mathbf{w}^n_{i,j,k} + \mathbf{w}^{n-1}_{i,j,k}}{2\Delta t} + \frac{\mathbf{R}_{i,j,k}\big(\mathbf{w}^{n+1,m}_{i,j,k}\big)}{V^{n+1}_{i,j,k}} = 0, \;\; (27)$$

where the m-th pseudo-time iterate at the real time step $n+1$ is denoted by $\mathbf{w}^{n+1,m}$ and the cell volumes are constant during the pseudo-time iteration. The unknown $\mathbf{w}^{n+1}_{i,j,k}$ is obtained when the first term in Equation (26) converges to a specified tolerance. An implicit scheme is used for the pseudo-time integration. The flux residual $\mathbf{R}_{i,j,k}\big(\mathbf{w}^{n+1}_{i,j,k}\big)$ is linearized as

$$\begin{aligned}
\mathbf{R}_{i,j,k}\big(\mathbf{w}^{n+1}\big) &= \mathbf{R}_{i,j,k}\big(\mathbf{w}^n_{i,j.k}\big) + \frac{\partial \mathbf{R}_{i,j,k}\big(\mathbf{w}^n_{i,j.k}\big)}{\partial t}\Delta t + O(\Delta t^2) \\
&\approx \mathbf{R}^n_{i,j,k}\big(\mathbf{w}^n_{i,j.k}\big) + \frac{\partial \mathbf{R}^n_{i,j,k}}{\partial \mathbf{w}^n_{i,j,k}}\big(\mathbf{w}^{n+1}_{i,j,k} - \mathbf{w}^n_{i,j,k}\big) \qquad (28)
\end{aligned}$$

Using this linearization in pseudo-time, Equation (27) becomes a sparse system of linear equations. For the solution of this system, the Conjugate Gradient method with a simple Jacobi pre-conditioner is used.

5.3   Time-dependent channel flow simulation

In this section, the flow in a square channel is considered. The mean flow direction is the x-direction, while the channel's lower and upper walls are placed at $z = 0\sigma$ and $z = 40\sigma$, respectively. The flow is assumed constant in the y-direction. The considered domain is 40σ long in all three coordinate direction. Although the flow is two-dimensional, a three-dimensional solution method is used here, hence the use of the constant y-direction. A finite-volume discretization method is used with a uniform mesh with 10 cells in both the $x-$ and the y-directions, while a stretched mesh with 20 cells is used in the z-direction.

The time-dependent problem starts from a steady flow established by a constant pressure gradient $dp/dx = -0.005$. From $t = 100$ to $t = 500$, this pressure gradient is then linearly increased to $dp/dx = -0.010$. The time-step used in the finite-volume method is $dt = 2$ (macro-scale time units). The Molecular Dynamics method is used in this example to evaluate the viscous stresses on the first 4 cell faces near both domain walls, i.e., the cell face on the solid wall and the first three faces away from the wall. Due to the homogeneity and periodicity of the flow, these 4 micro-scale solutions are similarly used for the whole $x - y$ planes for the near-wall cell layers. Due to the symmetry of the problem, these 'micro-scale' viscous are re-used for both the lower and upper domain walls. The remaining cell faces use a Newtonian fluid assumption for the viscous flux formulation, with the viscosity of the medium assumed constant at $\mu = 2.0$.

For the idealized case in which all cell faces use Newtonian viscous stresses, the solution of this flow problem is shown as the solid black line in Figure 2(a), where the velocity in the center of the domain is plotted versus time.

For the Lennard–Jones fluid considered in the Molecular Dynamics method, the density is assumed to be $0.80\sigma^{-3}$, while the temperature is $T = 1.50$. For these conditions, the Lennard–Jones fluid has a viscosity of around 2.03, i.e., very close to the assumed constant value in the Newtonian fluid part of the

computational domain. As discussed previously, the viscous stresses, as functions of the imposed velocity gradients, are computed using the Lees–Edwards boundary conditions. In the Molecular Dynamics simulations, ensemble averaging as well as temporal averaging is employed. Typically, 4 or 8 independent realizations for each shear-rate are constructed, which are then sampled through a sampling duration of typically 100 Lennard–Jones time units. For the MD time-step here, i.e., 0.001τ, this involves $100,000$ MD time steps.

5.4 Approximation of the statistical scatter in micro-scale problems

In the present paper, time-splitting methods are designed which can be regarded as extensions of the dual-time stepping method described in the previous sections. To facilitate this algorithm design process, it is important to reduce the computational cost of the present channel flow simulations, since in this process many different parameters will have to be evaluated. The most time-consuming part of the algorithms in the present paper is the micro-scale Molecular Dynamics shear stress evaluations. To reduce the computational cost of this investigation, the computationally expensive MD simulations are actually replaced by a modeled micro-scale viscous flux.

The aim of these model micro-scale problems is to provide an equivalent of the micro-scale MD viscous stresses for a given velocity gradient with a statistical scatter sampled from a random distribution. The amplitude of the random statistical scatter in the predicted micro-scale viscous stresses is derived from the actual MD data from the simulations of the previous section.

Figures 5 and 6 show the predicted apparent viscosity from the 24 time-steps at which a full MD viscous stress evaluation was conducted for the 4 cell faces nearest to the domain walls. The predicted apparent viscosities are plotted versus the sampling duration. Also shown are the average, as well as the L_2, L_4, and L_6 norms of the deviation from this average. Based on this data, an approximate statistical scatter as a function of the sampling duration is derived based on the L_6 norm, as shown in the figures.

6   Numerical Experiments: Splitting Methods for Coupled Micro–Macro System of Equations

In this section, three time-integration methods derived from the implicit dual-time stepping method are derived and evaluated for the time-dependent channel flow example problem.

6.1   Method 1: Fixed-interval micro-scale evaluations

In this first example, the coupling with the Molecular Dynamics method takes place by introducing a correction to the Newtonian shear stresses for the cell faces with an associated micro-scale MD shear stress evaluation, as presented in Equation (24). This method has the following steps:

- for time step $<= 100$, the solution is marched forward in time using the Newtonian shear stresses evaluation employed throughout the domain

- at time step 20, 40, 60, 80 and 100, micro-scale MD problems are constructed for the 4 cell faces nearest to the domain walls. For each cell face, 4 independent realizations are created, while the viscous stresses are sampled over 100τ after an initial equilibration stage of 50τ.

- for time steps > 100, the viscous fluxed in the 4 cell faces nearest to the domain walls are corrected using an apparent viscosity derived from averaging over the last 5 MD evaluations for each cell face

- every 20 time steps, another set of micro-scale MD problems are constructed based on the current cell face velocity gradient, and following a new set of MD viscous stress evaluations, the 'averaged apparent' viscosity is updated.

The above method is a simple method of taking into account the shear-rate dependence of the apparent viscosity, while greatly reducing the computational overhead compared to a full set of MD shear stress evaluations computed for each macro-scale time step. However, for rapidly changing macro-scale velocity

gradients, using the 'running' average of the latest MD predictions with a number of previous evaluations introduces a potential time-lag in incorporating the shear-rate dependence of the apparent viscosity.

The method can be summarized as follows:

Algorithm 6.1. *On a uniform time grid with $t^n = t_0 + n\Delta t$, $n = 0, \ldots, N$, (where N is given), the discretized coupled macro- and micro-scale equations are integrated in time from time level n to $n+1$ using the following scheme:*

1) *initialize the averaged apparent viscosity $\mu_{ave} = \mu_{approx}$*

2) *if $n < 100$ and n is multiple of $n_{interval}$ go to 3) else go to 4)*

3) *dual-time step update based on fixed μ_{ave}*

    i) *for the cell faces with micro-scale fluxes, compute the velocity gradients*

    ii) *construct the viscous flux corrections f_i using the updated apparent viscosity*

    iii) *perform dual-time step update using n_{Newton} relaxation steps.*

4) *dual-time step update based on updated μ_{ave}*

    i) *for the cell faces with micro-scale fluxes, compute the velocity gradients*

    ii) *initialize the Molecular Dynamics micro-scale problems with the imposed velocity gradients from the finite-volume cell faces and integrate these through the initial equilibration phase (e.g., $t_{equi} = 50\tau$)*

    iii) *integrate micro-scale problems in time through t_{sample} micro-scale time and average apparent viscosity in time and ensemble average over $n_{ensemble}$ independent realizations*

    iv) *compute new μ_{ave} as average over last n_{window} (including present) Molecular Dynamics solutions*

    v) *construct the viscous flux corrections f_i using updated apparent viscosity*

    vi) *perform dual-time step update using n_{Newton} relaxation steps.*

if n < N go to 1)

Figure 2 presents the results for the velocity predicted with the above method from two independent realizations. Compared to the idealized case with Newtonian fluxes throughout the domain, the use of MD micro-scale fluxes leads to a small reduction in the cell center velocity, since the apparent viscosity predicted by the MD simulations is slightly higher than the constant viscosity used in the remainder of the domain. Also, by averaging over 5 evaluations, the statistical scatter in the MD micro-scale fluxes leads to only modest fluctuations in the macro-scale velocity field compared to the fully Newtonian case.

The predicted apparent viscosity and the resulting 'running averages' are presented in Figure 3, clearly showing the significant reduction of the statistical scatter in the MD data when such an averaging is used in addition to the already used temporal and ensemble averaging.

The present dual-time stepping method solves a 'quasi-steady' state problem at each time step. For each of these quasi-steady state problems, an implicit solution method is used based on an under-relaxed Newtonian relaxation process. The convergence of this implicit system for a certain number of time-steps is presented in Figure 4. In the examples shown, 25 'pseudo-steps' are used, leading to a reduction of the maximum norm of the residual (which now includes the 'unsteady' flow contribution) of at least 6 orders of magnitude. When this residual norm is reduced to machine precision, the only discretization errors due to the time discretization are those due to the truncation errors in the employed implicit 3-point stencil. With a reduction of the residual norm of 6 or 7 orders of magnitude, it can be expected that the additional contributions are much smaller than the truncation errors in the implicit 3-point stencil.
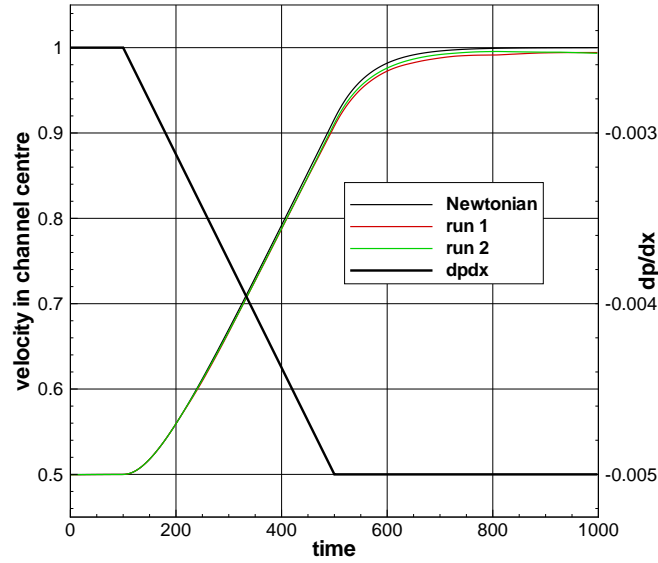
(a) Velocity in channel center
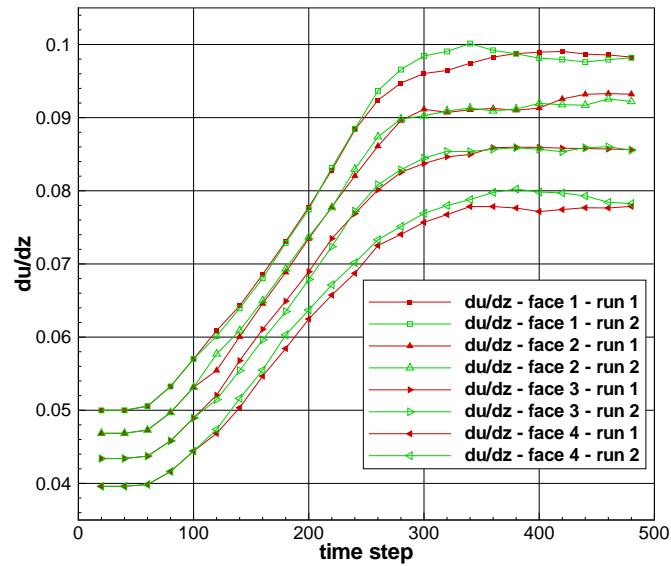
(b) Velocity gradients near walls

Figure 2: Channel flow with time-dependent pressure gradient. Dual-time stepping method with averaging of apparent viscosity. Finite-volume discretization method with Molecular Dynamics viscous fluxes on first 4 cells near lower and upper walls. Lennard–Jones fluid at $0.80\sigma^{-3}$ and $T = 1.50$. MD data averaged over 4 realizations, $\tau_{sample} = 100$.
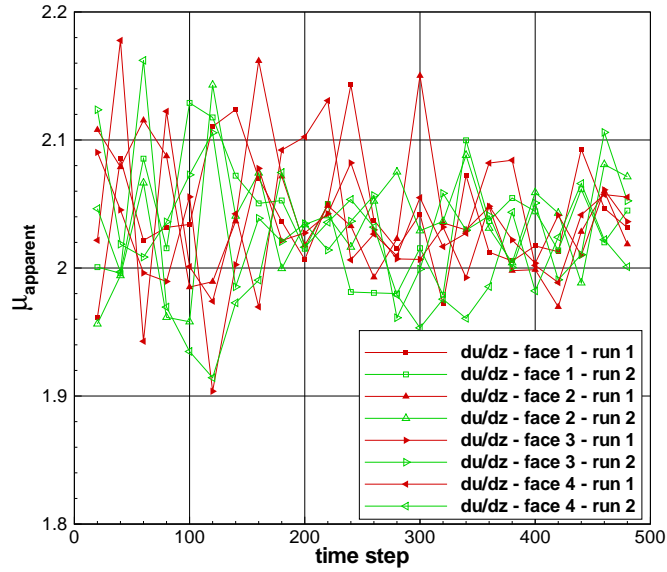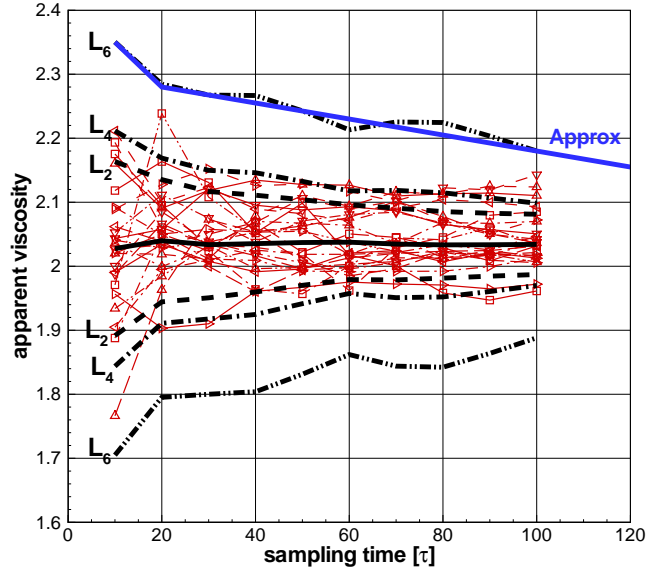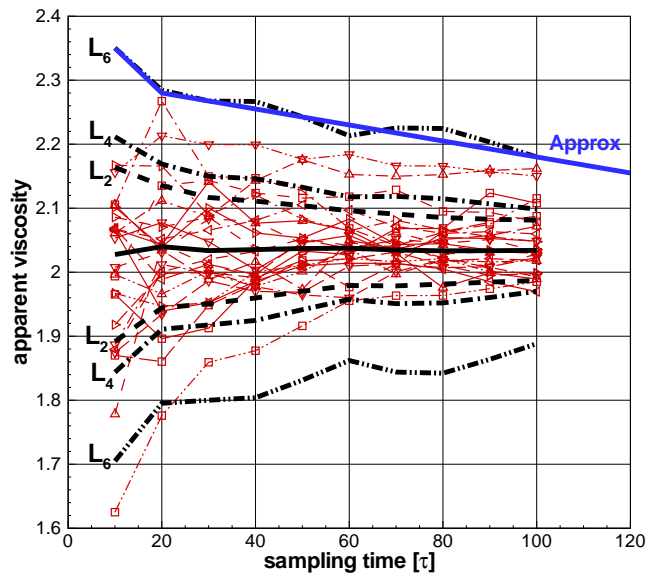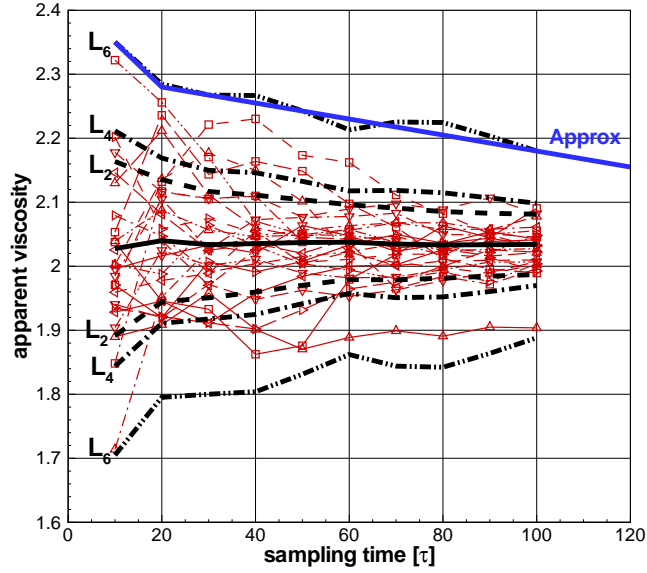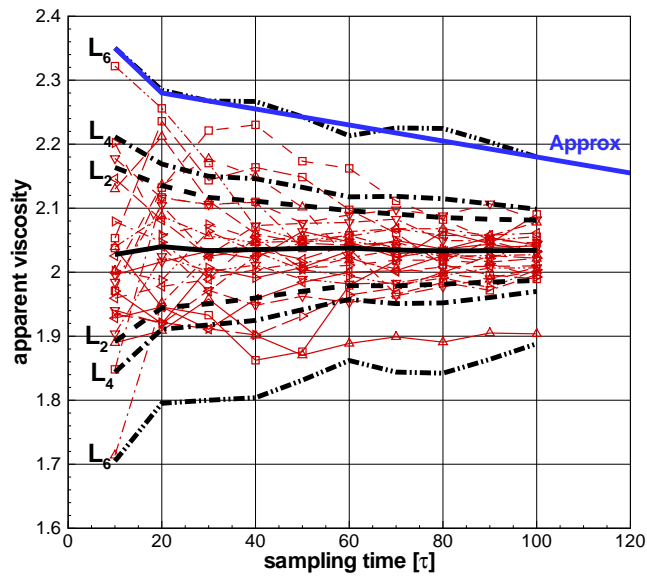
(a) apparent viscosity
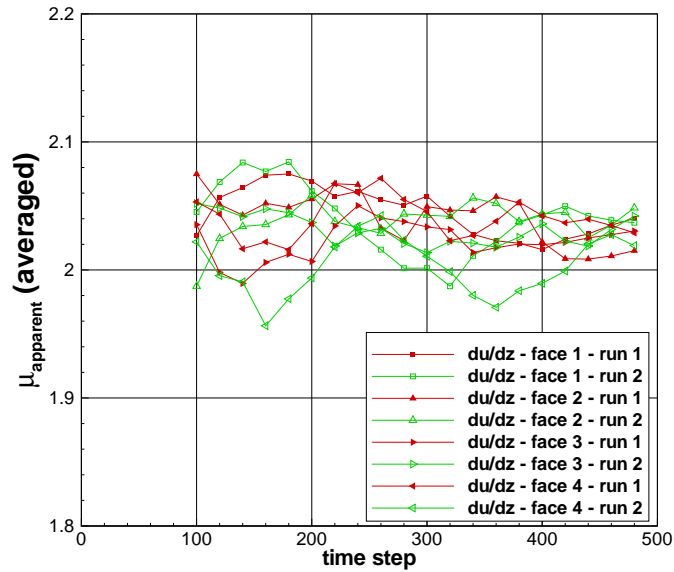
(b) averaged apparent viscosity

Figure 3: Channel flow with time-dependent pressure gradient. Dual-time stepping method with averaging of apparent viscosity. Finite-volume discretization method with Molecular Dynamics viscous fluxes on first 4 cells near lower and upper walls. Lennard–Jones fluid at $0.80\sigma^{-3}$ and $T = 1.50$. MD data averaged over 4 realizations, $\tau_{sample} = 100$.
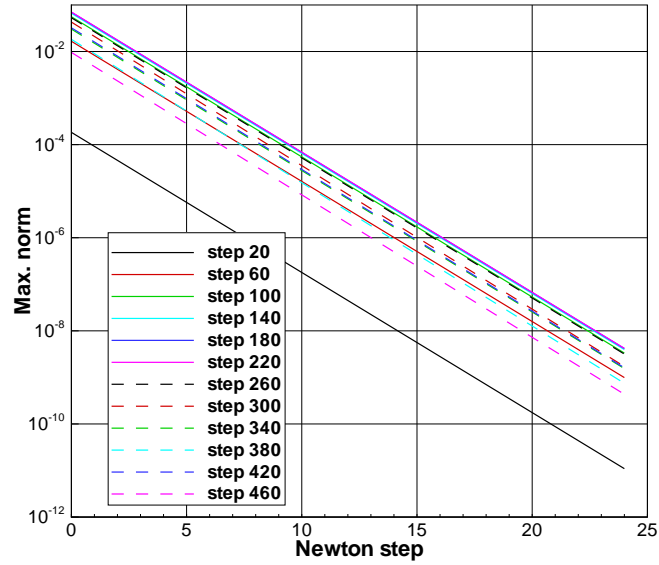
(a) realization 1
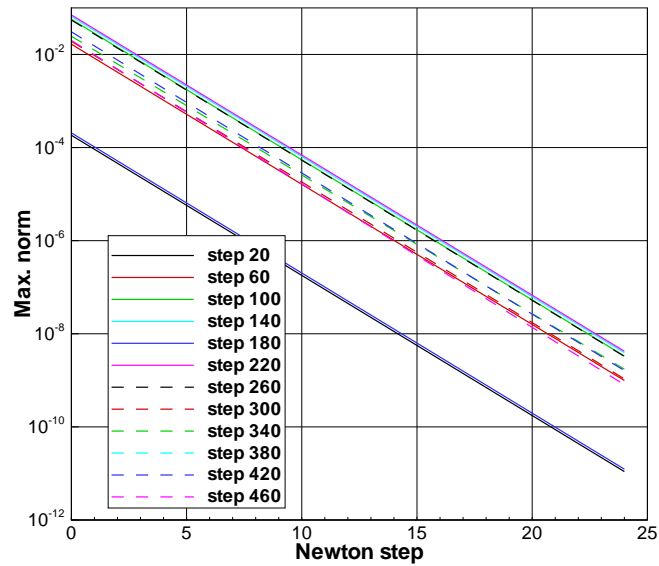
(b) realization 2

Figure 4: Channel flow with time-dependent pressure gradient. Dual-time stepping method with averaging of apparent viscosity. Convergence of 'inner-loop' in dual-time step method. Channel flow with time-dependent pressure gradient. Lennard–Jones fluid at $0.80\sigma^{-3}$ and $T = 1.50$. MD data averaged over 4 realizations, $\tau_{sample} = 100$.

(a) face 1

(b) face 2

Figure 5: Convergence of predicted apparent viscosities in 4 cell faces as function of sampling time. Lennard–Jones fluid at $0.80\sigma^{-3}$ and $T = 1.50$. MD data averaged over 4 realisations, $10 <= \tau_{sample} <= 100$.

(a) face 3

(b) face 4

Figure 6: Convergence of predicted apparent viscosities in 4 cell faces as function of sampling time. Lennard–Jones fluid at $0.80\sigma^{-3}$ and $T = 1.50$. MD data averaged over 4 realizations, $10 <= \tau_{sample} <= 100$.

6.2 Method 2: Dual-time stepping method with fixed-point iteration

In this second method, the coupling with the Molecular Dynamics method takes place by introducing a correction to the Newtonian shear stresses for the cell faces with an associated micro-scale MD shear stress evaluation, as presented in Equation (24). In this method, the following steps are used:

- for time step $<= 100$, the solution is marched forward in time using the Newtonian shear stresses evaluation employed throughout the domain

- for time steps > 100, the viscous fluxes in the 4 cell faces nearest to the domain walls are corrected by data derived from Molecular Dynamics micro-scale problems. For each cell face, 4 independent realizations are created, followed by an initial equilibration stage of 50τ and an initial sampling time of 10τ. Using the MD predictions, the dual-time stepping method is used to create the velocity field for fixed-point iteration 0,

- for fixed-point iteration $1, \ldots, n$, the MD micro-scale solutions are integrated for a further 10τ sampling durations. With the updated MD predictions, the dual-time stepping method is used to create the velocity field for this fixed-point iteration.

In this method, the number of fixed-point iterations is assumed to be constant. The method can be summarized as follows:

Algorithm 6.2. *On a uniform time grid with $t^n = t_0 + n\Delta t$, $n = 0, \ldots, N$, (where N is given), the discretized coupled macro- and micro-scale equations are integrated in time from time level n to $n + 1$ using the following scheme:*

1) For the cell faces with micro-scale fluxes, compute the velocity gradients

2) Initialize the Molecular-Dynamics micro-scale problems with the imposed velocity gradients from the finite-volume cell faces and integrate these through the initial equilibration phase (e.g., $t_{equi} = 50\tau$)

3) Dual-time step with fixed-point iteration. Perform the following steps:

i) set fixed point counter $iter = 0$

    ii) integrate micro-scale problems in time through an additional 10τ and sample apparent viscosity through total micro-scale sampling time and ensemble average over $n_{ensemble}$ independent realizations

    iii) construct the viscous flux corrections f_i using updated apparent viscosity

    iv) perform dual-time step update using n_{Newton} relaxation steps

   *v) if iter $< n_{fp}$, increment iter and go to i)*

if $n < N$ go to 1).

In the next section, a more adaptive method is formulated, which adjusts the number of fixed-point iterations to an appropriate error norm on both viscous flux corrections and velocity field updates.

In this section, the expensive MD simulations are replaced with a modeled micro-scale scale prediction for the apparent viscosity.

$$\mu_{apparent} \quad = \quad 2.03 + \mu_{scatter}(t_{sampling})rand() \tag{29}$$

The statistical scatter amplitude is shown in Figures 5 and 6, with a linear continuation to zero scatter for sampling times exceeding 200τ. Clearly, this is an idealized situation, but allows an initial assessment of the time-splitting methods developed in the present paper.

In the examples presented here, 10 fixed point iterations lead to a statistical scatter in the predicted micro-scale viscosities of similar magnitude as the full MD sampling over 100τ used in the previous section. For 20 fixed point iterations and more, the statistical scatter is removed completely, leading to a constant viscous flux correction due to the fact that the modeled value of 2.03 is slightly higher than the constant value used in the Newtonian shear stress evaluation.
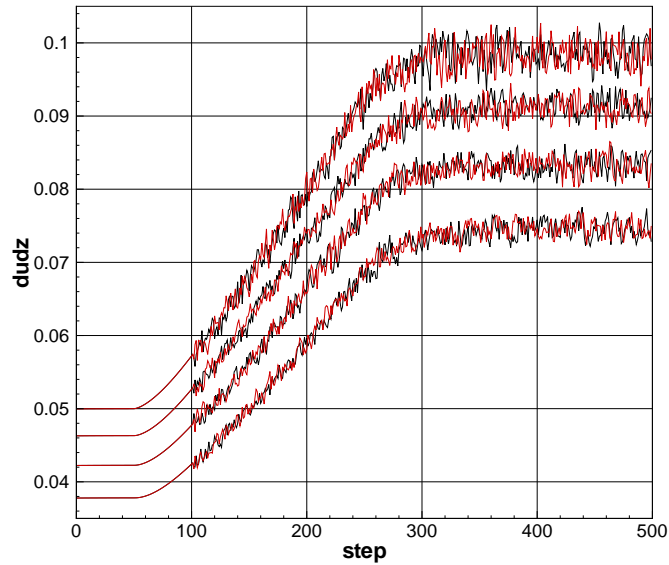
(a) Velocity gradients near walls - 10 fixed-point inner iterations
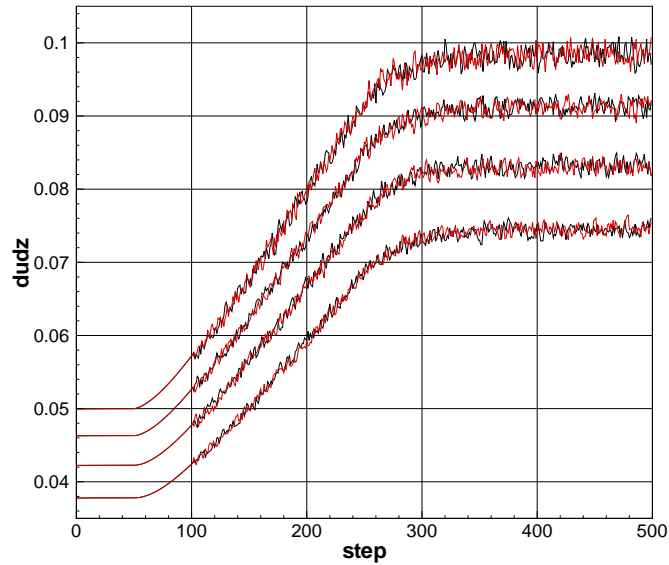
(b) Velocity gradients near walls - 15 fixed-point inner iterations

Figure 7: Channel flow with time-dependent pressure gradient. Dual-time stepping method with fixed-point iteration in MD sampling of apparent viscosity. Finite-volume discretization method with approximated statistical scatter of Molecular Dynamics viscous fluxes as function of sampling duration on first 4 cells near lower and upper walls.

6.3   Method 3: Adaptive fixed-point iteration

The final method presented here is based on an adaptive splitting approach, i.e., one which truncates the fixed-point iteration whenever the viscous flux corrections and/or the velocity field updates relative to the previous fixed point iterations fall below a certain threshold. In this respect, it is a modified version of the algorithm used in the previous section. The method can be summarized as follows:

Algorithm 6.3. *On a uniform time grid with $t^n = t_0 + n\Delta t$, $n = 0, \dots, N$, (where N is given), the discretized coupled macro- and micro-scale equations are integrated in time from time level n to $n + 1$ using the following adaptive scheme:*

1) *For the cell faces with micro-scale fluxes, compute the velocity gradients*

2) *Velocity gradient criterion: $max\left(\left|\left(\frac{\partial u_i}{\partial x_j}\right)^n_{micro} - \left(\frac{\partial u_i}{\partial x_j}\right)^{last}_{micro}\right|\right) > crit_{grad}$, $crit_{grad} \in \mathbb{R}^+$. If criterion is satisfied goto 3) else 4)*

3) *Dual-time step with fixed-point iteration. Perform the following steps:*

    i) *Using the last estimate of the micro-scale apparent viscosity, compute an estimate of the updated velocity field at the present time step using dual-time step update.*

    ii) *Compute the velocity normalization factor as: $u_{norm} = max(\tilde{u}_i(t^{n+1} - u_i(t^n)$, where $\tilde{u}$ denotes the estimated velocity from step i)*

    iii) *Compute viscous flux correction normalization $f_{norm} = max(\tilde{f}_i(t^{n+1})$, with $\tilde{f}$ the viscous flux correction based on the last apparent viscosity computation*

    iv) *Store micro-scale velocity gradients: $\left(\frac{\partial u_i}{\partial x_j}\right)^{last}_{micro} = \left(\frac{\partial u_i}{\partial x_j}\right)^n_{micro}$*

    v) *Initialize the Molecular-Dynamics micro-scale problems with the imposed velocity gradients from the finite-volume cell faces and integrate these through the initial equilibration phase (e.g., $t_{equi} = 50\tau$)*

    vi) *Fixed-point iteration:*

a) integrate micro-scale problems in time through an additional 10τ and sample apparent viscosity through total micro-scale sampling time and ensemble average over $n_{ensemble}$ independent realizations

b) construct the viscous flux corrections f_i using updated apparent viscosity

c) perform dual-time step update using n_{Newton} relaxation steps

d) check convergence of fixed-point iteration using the stop criterion $\left|u_i(t^{n+1}) - u_{i-1}(t^{n+1}\right|/u_{norm} \leq err_u$, $err_u \in \mathbb{R}^+$ and/or $\left|f_i(t^{n+1}) - f_{i-1}(t^{n+1}\right|/f_{norm} \leq err_f$, $err_f \in \mathbb{R}^+$

e) if criterion is satisfied, time step is completed, else go to step a)

4) Dual-time step without fixed-point iteration.

i) Using the last estimate of the micro-scale apparent viscosity, compute flux corrections f_i

ii) Perform dual-time step update using n_{Newton} relaxation steps.

if $n < N$ go to 1).

In the present dual-time step formulation, each fixed-point iteration corresponds to the solution of a 'pseudo-steady' state problem using a Newton relaxation method, as discussed previously. For each increment of the fixed-point iteration counter, the micro-scale problem is marched forward by a pre-defined time-increment (in the present section, 10 Lennard–Jones time units) and the updated viscous flux correction will be checked with that at the previous iteration, while after the solution for the velocity field for iteration, also the convergence of the velocity field relative to the previous iteration is checked.

Table 1: Truncation criteria used in method 3

Criterion	$crit_{grad}$	err_u	err_f	fixed-point truncation
1A	0.05	0.25	0.25	or
1B	0.05	0.25	0.25	and
2A	0.05	0.50	0.50	or
2B	0.05	0.50	0.50	and

7   Conclusions and Discussion

We present an optimization of coupling Navier–Stokes and Molecular Dynamics simulation by applying iterative operator-splitting methods. We discussed different techniques to reduce costly molecular dynamical computations by averaging, by using microscale models, and by using adaptive iterations. Iterative and adaptive iterative splitting methods can simplify the coupling process and yield the same results as from using costly computations. Here we have presented an accelerated solver with simultaneous coupling schemes. In the future, we will present more improved algorithms involving multi-grid schemes and nonlinear schemes.

References

[1] M. Allen, D. Tildesly, *Computer Simulation of Liquids*, Clarendon Press, Oxford, 1987.

[2] H. Berendsen, J. Postma, W. van Gunsteren, A. Dinola and J. Haak, Molecular-Dynamics with Coupling to an External Bath, *J. Chem. Phys.*, **81**, (1984), 3684–3690.

[3] P. Csomós, I. Faragó and A. Havasi, Weighted sequential splittings and their analysis, *Comput. Math. Appl.*, (to appear).

[4] K.-J. Engel and R. Nagel, *One-Parameter Semigroups for Linear Evolution Equations*, Springer-Verlag, New York, 2000.

[5] R.E. Ewing, Up-scaling of biological processes and multiphase flow in porous media, *IIMA Volumes in Mathematics and its Applications*, Springer-Verlag, **295**, (2002), 195–215.

[6] I. Farago, Splitting methods for abstract Cauchy problems, *Lect. Notes Comp. Sci.*, Springer-Verlag, Berlin, **3401**, (2005), 35–45.

[7] I. Farago and J. Geiser, *Iterative Operator-Splitting methods for Linear Problems*, Preprint No. 1043 of the Weierstrass Institute for Applied Analysis and Stochastics, Berlin, June 2005.

[8] I. Farago and A. Havasi, *On the Convergence and Local Splitting Error of Different Splitting Schemes*, Eötvös Lorand University, Budapest, 2004.

[9] P. Frolkovič and J. Geiser, Numerical Simulation of Radionuclides Transport in Double Porosity Media with Sorption, *Proceedings of Algorithmy 2000, Conference of Scientific Computing*, (2000), 28-36.

[10] J. Geiser, Operator-Splitting Methods in Respect of Eigenvalue Problems for Nonlinear Equations and Applications to Burgers Equations, *Journal of Computational and Applied Mathematics*, Elsevier, Amsterdam, (accepted May, 2009).

[11] J. Geiser, Iterative Operator-Splitting Methods with higher order Time-Integration Methods and Applications for Parabolic Partial Differential Equations, *Journal of Computational and Applied Mathematics*, Elsevier, Amsterdam, The Netherlands, **217**, (2008), 227–242.

[12] J. Geiser, Numerical Simulation of a Model for Transport and Reaction of Radionuclides, *Proceedings of the Large Scale Scientific Computations of Engineering and Environmental Problems, Sozopol, Bulgaria*, (2001).

[13] W. Hundsdorfer and L. Portero, A Note on Iterated Splitting Schemes, *CWI Report MAS-E0404*, Amsterdam, Netherlands, (2005).

[14] W.H. Hundsdorfer and J. W. Verwer *Numerical solution of time-dependent advection-diffusion-reaction equations*, Springer-Verlag, Berlin, 2003.

[15] J. Irving and J. Kirkwood, The Statistical Mechanical Theory of Transport Processes IV, J. Chem. Phys., 18, (1950), 817–829.

[16] A. Jameson, Time Dependent Calculations Using Multigrid, with Applications to Unsteady Flows past Airfoils and Wings, *10th Computational Fluid Dynamics Conference*, Honolulu, Hawai, AIAA Paper **1991-1596**, (June 24-26, 1991).

[17] J. Kanney, C. Miller and C. Kelley, Convergence of iterative split-operator approaches for approximating nonlinear reactive transport problems, *Advances in Water Resources*, **26**, (2003), 247–261.

[18] P. Van Leemput, W. Vanroose and D. Roose, Mesoscale analysis of the equation-free constrained runs initialization scheme, *Multiscale Model. Simul. Model.*, **6**(4), (2008), 1234–1255.

[19] A. Lees and S. Edwards, The Computer Study of Transport Processes under Extreme Conditions, *J. Phys. C*, **5**, (1972), 1921–1929.

[20] J. Lennard–Jones, Cohesion, *Proc. Phys. Soc.*, **43**, (1931), 461–482.

[21] J. Van Lent, *Multigrid Methods for Time-Dependent Partial Differential Equations*, PhD Thesis, Katholieke Universiteit Leuven, Leuven, Belgium, 2006.

[22] R.J. LeVeque, *Finite Volume Methods for Hyperbolic Problems*, Cambridge Texts in Applied Mathematics, 2002.

[23] G. Marchuk, Some applicatons of splitting-up methods to the solution of problems in mathematical physics, *Aplikace Matematiky*, **1**, (1968) 103–132.

[24] R. Steijl and G. Barakos, Coupled Navier–Stokes - Molecular dynamics simulations using a multi-physics flow simulation framework, *International Journal for Numerical Methods in Fluids*, Wiley, published online, (2009).

[25] G. Strang, On the construction and comparision of difference schemes, *SIAM J. Numer. Anal.*, **5**, (1968), 506–517.

[26] S. Vandewalle, *Parallel Multigrid Waveform Relaxation for Parabolic Problems*, Teubner, Stuttgart, 1993.

[27] L. Verlet, Computer Experiments of Classical Fluids I: Thermodynamical Properties of Lennard-Jones Molecules, *Physical Review*, **159**, (1967) 98.

[28] J. Verwer and B. Sportisse, A note on operator splitting in a stiff linear case, *MAS-R9830*, (1998).

[29] Z. Zlatev, *Computer Treatment of Large Air Pollution Models*, Kluwer, 1995.
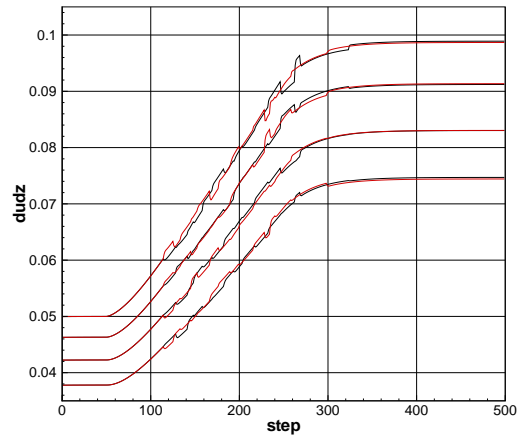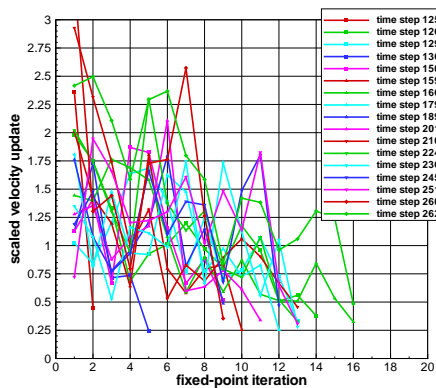
(velocity field)
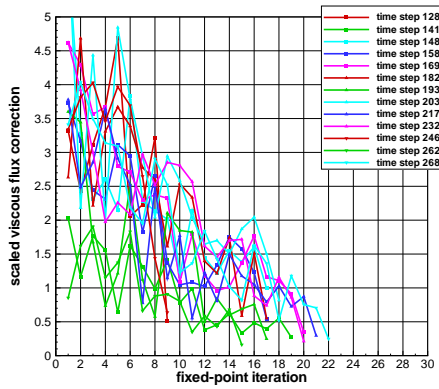
(b) run 1 - viscous flux correction
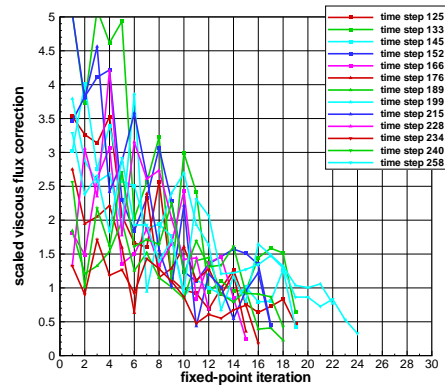
(c) run 2 - viscous flux correction
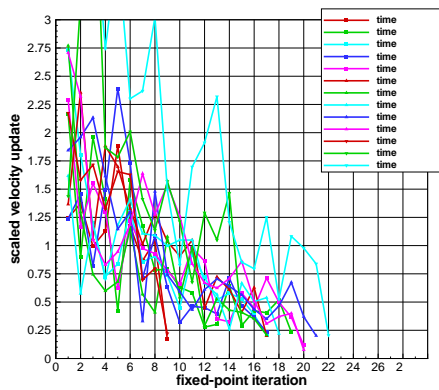
(d) run 1 - velocity update
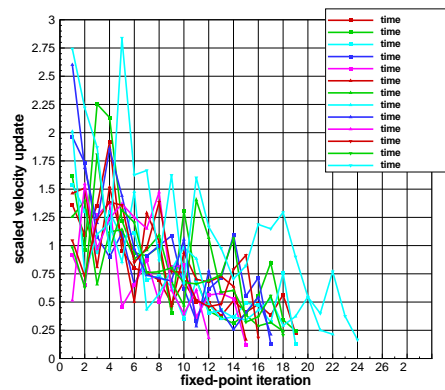
(e) run 2 - velocity update

Figure 8: Adaptive fixed-point scheme with truncation criteria 1A. Dual-time stepping method with adaptive MD sampling time in inner iterations. Finite-volume discretization with micro-scale viscous fluxes on first 4 cells near lower and upper walls. Approximate statistical scatter of Molecular Dynamics fluxes.
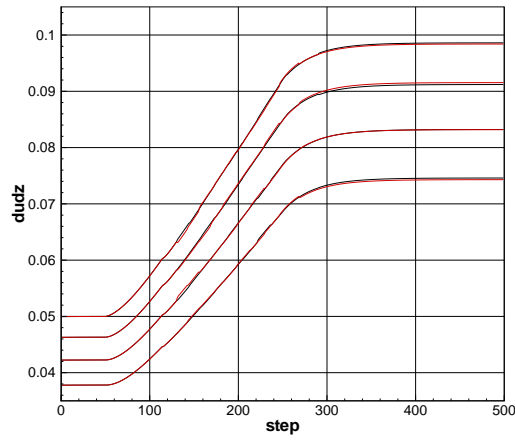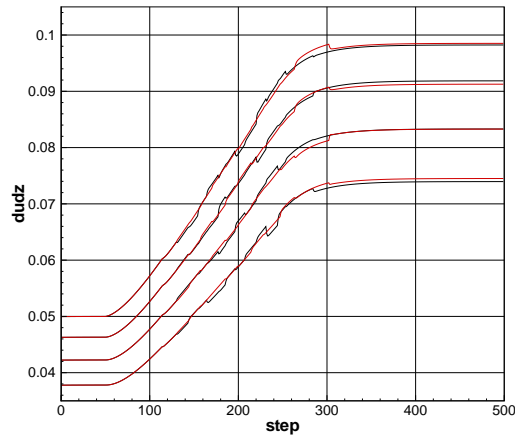
(velocity field
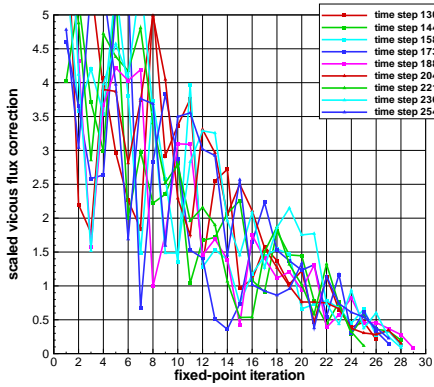
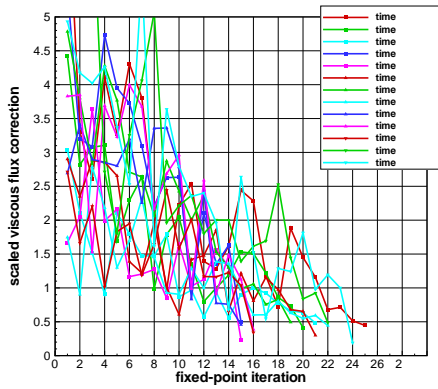(b) run 1 - viscous flux correction   (c) run 2 - viscous flux correction
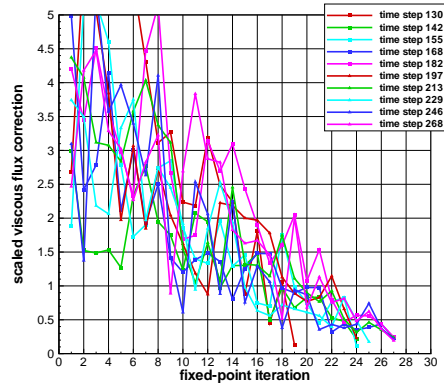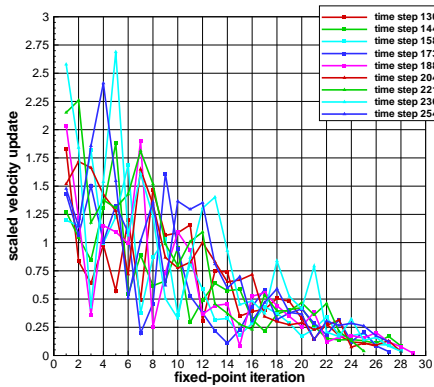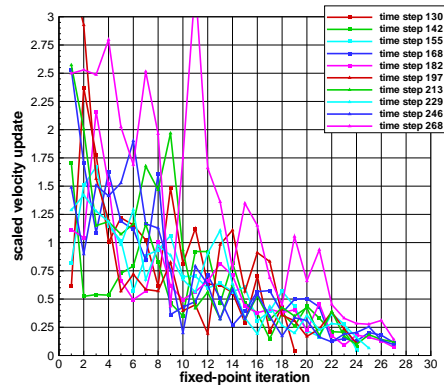
(d) run 1 - velocity update   (e) run 2 - velocity update

Figure 9: Adaptive fixed-point scheme with truncation criteria. Dual-time stepping method with adaptive MD sampling time in inner iterations. Finite-volume discretization with micro-scale viscous fluxes on first 4 cells near lower and upper walls. Approximate statistical scatter of Molecular Dynamics fluxes.
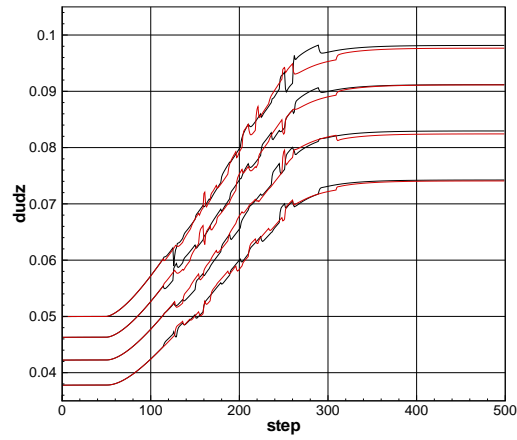
(velocity field
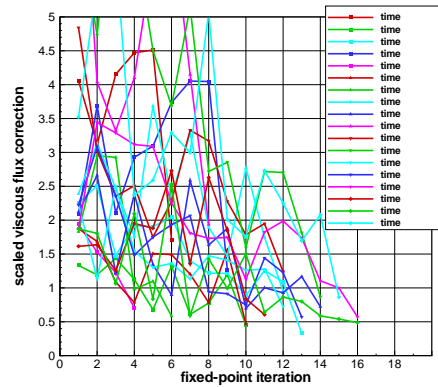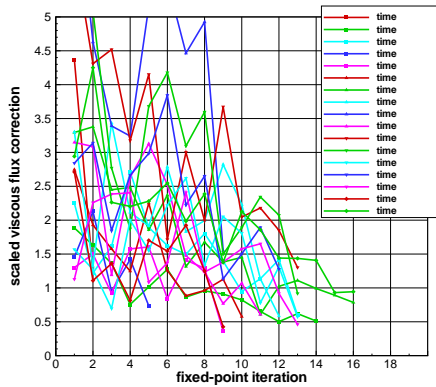
(b) run 1 - viscous flux correction   (c) run 2 - viscous flux correction
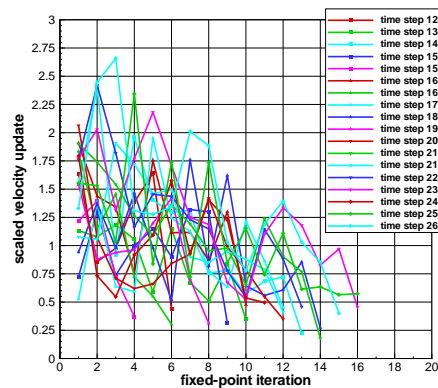
(d) run 1 - velocity update   (e) run 2 - velocity update
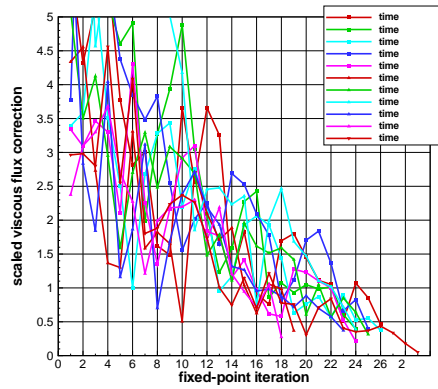
Figure 10: Adaptive fixed-point scheme with truncation criteria 2A. Dual-time stepping method with adaptive MD sampling time in inner iterations. Finite-volume discretization with micro-scale viscous fluxes on first 4 cells near lower and upper walls. Approximate statistical scatter of Molecular Dynamics fluxes.
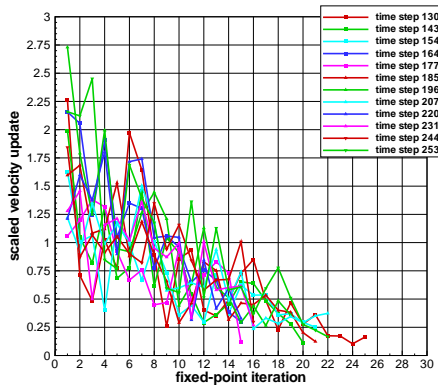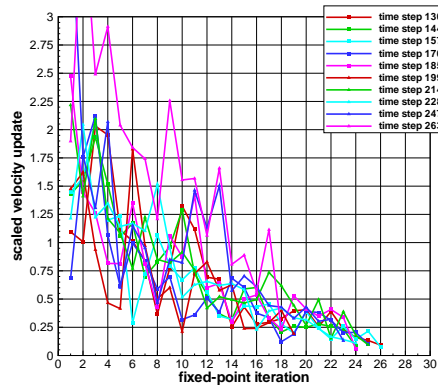
(a) velocity field

(c) run 1 - viscous flux correction

(d) run 2 - viscous flux correction

(e) run 1 - velocity update

(f) run 2 - velocity update

Figure 11: Adaptive fixed-point scheme with truncation criteria 2B. Dual-time stepping method with adaptive MD sampling time in inner iterations. Finite-volume discretization with micro-scale viscous fluxes on first 4 cells near lower and upper walls. Approximate statistical scatter of Molecular Dynamics fluxes.